发光学报
CHINESE JOURNAL OF LUMINESCENCE
中文核心期刊
主管：中国科学院
主办：中国科学院长春光学精密机械与物理研究所
中国物理学会发光分会
主编：申德振

一种新型交联电子传输材料在OLED中的应用

高朝， 谢黎明， 苏文明， 崔铮

引用本文:
高朝, 谢黎明, 苏文明, 等. 一种新型交联电子传输材料在OLED中的应用[J]. 发光学报, 2020, 41(9): 1093-1101.
GAO Zhao, XIE Li-ming, SU Wen-ming, et al. Application of A Novel Cross-linkable Electron Transport Material in OLED[J]. *Chinese Journal of Luminescence*, 2020, 41(9): 1093-1101.

在线阅读 View online: https://doi.org/10.37188/fgxb20204109.1093

Article ID: 1000-7032(2020)09-1093-09

Application of A Novel Cross-linkable Electron Transport Material in OLED

GAO Zhao[1,2], XIE Li-ming[1], SU Wen-ming[1*], CUI Zheng[1,2]

(1. *Printable Electronics Research Center, Suzhou Institute of Nano-Tech and Nano-Bionics, Chinese Academy of Sciences, Suzhou* 215123, *China*;
2. *School of Physical Science and Technology, Shanghai Tech University, Shanghai* 201210, *China*)

* *Corresponding Author, E-mail: wmsu*2008@ *sinano. ac. cn*

Abstract: A new cross-linkable electron transport layer(ETL) material, 2,4,6-tris(4′-vinyl-[1,1′-biphenyl]-3-yl)-1,3,5-triazine(TV-T2T) was designed and synthesized. The film formation of the cross-linkable material TV-T2T has the excellent solvent resistance. The lowest unoccupied molecular orbital(LUMO) level of TV-T2T is −3.5 eV, which could deliver efficient charge injection from the zinc oxide(ZnO) to the emission layer. In addition, the surface roughness of 2.27 nm in the film of triple-layer ZnO/TV-T2T/2,6-Dczppy: $Ir(mppy)_3$, is lower than that of the film without TV-T2T(2.39 nm), resulting in a reduced leakage current. The solution-processed inverted OLED with ETL material TV-T2T, achieved an EQE of 5.1% compared to the 3.0% EQE of the device without TV-T2T layer, demonstrating an improvement of 1.7-fold for the inverted OLEDs.

Key words: cross-linkable material; electron transport layer; electron injection property; solution processing; inverted organic light emitting diodes

CLC number: O482.31 **Document code**: A **DOI**: 10.37188/fgxb20204109.1093

一种新型交联电子传输材料在 OLED 中的应用

高 朝[1,2], 谢黎明[1], 苏文明[1*], 崔 铮[1,2]

(1. 中国科学院苏州纳米技术与纳米仿生研究所 印刷电子技术研究中心, 江苏 苏州 215123;
2. 上海科技大学 物质科学与技术学院, 上海 201210)

摘要: 设计并合成了一种新型的可交联电子传输材料 TV-T2T。该材料经过热交联之后具有优异的抗溶剂特性,并且 TV-T2T 的 LUMO 能级为 −3.5 eV,这将更有利于电子从 ZnO 层注入到发光层中。另外,溶液法制备的三层薄膜 ZnO/TV-T2T/2,6-Dczppy: $Ir(mppy)_3$,其粗糙度低至 2.27 nm,优于未加入 TV-T2T 电子传输层的双层薄膜(2.37 nm),可以有效减少漏电流的产生。随后,将 TV-T2T 应用于三层溶液法制备的倒置有机发光二极管中,获得了 5.1% EQE 的器件性能,是不加 TV-T2T 的器件性能(EQE 为 3.0%)的 1.7 倍。

关 键 词: 交联材料; 电子传输层; 电子注入能力; 溶液法; 倒置 OLED

收稿日期: 2020-06-18; **修订日期**: 2020-07-06
基金项目: 国家重点研发计划(2016YFB0401600)资助项目
Supported by National Key Research and Development Program of China(2016YFB0401600)

1 Introduction

In recent years, organic light emitting diodes (OLEDs) have attracted a great deal of attentions in academia and industry since it was invented by C W Tang[1] more than 30 years ago. Vacuum evaporation deposition[2-7] of small molecular materials has been dominant in the past 30 years for OLED manufacturing. However, due to the disadvantage of high cost and low material usage in the vacuum evaporation process, solution processed materials which mainly relying on spin coating[8] and inkjet printing[9-12] deposition processes, have been actively pursued. Besides, the interlayer erosion has been a major obstacle in solution-processed OLEDs. There are two main approaches to solve the problem, using orthogonal solvents[13-17] or cross-linkable materials[18-21]. The use of cross-linkable materials has advantages of high air stability and could favor more compact film formation[22], and a number of cross-linkable materials have been developed[23-26].

When OLEDs are used for display applications, passive-matrix OLEDs (PMOLEDs)[27] and active-matrix OLEDs (AMOLEDs) are the two main types[28-30]. For AMOLEDs, the light emission of each pixel is controlled by a number of thin film transistors (TFTs), which could potentially block the light emission on display panel. Owing to this, OLED with inverted structure takes an advantage of that the TFTs are made beneath the OLED pixels. However, the inverted OLED has the problem of highly efficiently injecting electrons from metal electrode to light emission layer. So, the electron material is very important to the inverted OLED. Many excellent electron materials have been reported[31-34]. Among them, triazine based compounds have been widely used as the electron transport layers[35-42]. Particularly, 2,4,6-tri([1,1′-biphenyl]-3-yl)-1,3,5-triazine (T2T) has been chosen as the ETL for its good electron transporting ability[43-44]. Nevertheless, T2T as a small molecular material, is insoluble and only suitable for vacuum evaporation deposition, which is not compatible with solution processing.

In this work, a modified version of T2T, the 2,4,6-tris(4′-vinyl-[1,1′-biphenyl]-3-yl)-1,3,5-triazine (TV-T2T), has been designed and synthesized. TV-T2T has good solubility and cross-linkable unit while maintains the advantages of T2T as well. The lowest unoccupied molecular orbital (LUMO) of TV-T2T is −3.5 eV, lying between the LUMO levels of ZnO (−4.0 eV) and 2,6-bis(3-(carbazol-9-yl)phenyl)pyridine (2,6-Dczppy) (−2.6 eV): tris(2-(4-tolyl)phenylpyridine) iridium ($Ir(mppy)_3$) (−2.4 eV), indicating that the TV-T2T would facilitate efficient charge transport. The surface roughness of ZnO/2,6-Dczppy: $Ir(mppy)_3$ and ZnO/TV-T2T/2,6-Dczppy: $Ir(mppy)_3$ have been measured to be 2.39 nm and 2.27 nm respectively. The thermodynamic property, photo-physical property, charge mobility and resistance to solvent erosion for TV-T2T were fully investigated. Tri-layer solution processing OLEDs were fabricated with the structure of ZnO/TV-T2T/2,6-Dczppy: $Ir(mppy)_3$. A maximum 5.1% EQE of OLEDs with the cross-linkable material TV-T2T has been achieved, comparing to the 3.0% EQE of the device without TV-T2T layer, delivering 1.7-fold of improvement.

2 Experiments

2.1 General Information

The elemental analysis (EA) was performed using vario Micro cube. The ^1H and ^{13}C NMR in the $CDCl_3$ spectra were obtained with a Bruker NMR spectrometer. Thermogravimetric analysis (TGA) was measured with the NETZSCH TG 209 F1 (Germany) on the condition of the nitrogen atmosphere by heating sample from 25 ℃ to 300 ℃ at the heating rate of 10 ℃/min. Differential scanning calorimetry (DSC) was used to investigate the TV-T2T of the thermodynamic stability with NETZSCH DSC 200F3 MAIA (Germany) at a heating rate of 10 ℃/min from room temperature to 300 ℃ under the nitrogen atmosphere. The ultraviolet-visible (UV) absorption and the photoluminescence (PL) spectra were performed on the Perkin-Elmer Lambda 750 spectrophotometer and a Hitachi F-4600 fluorescence spectrophotometer, respectively. Atom Force Microscopy (AFM) images were obtained with a veeco

Dimension 3100 at the ambient temperature in the tapping mode. The current-voltage (*I-V*) and luminance-voltage (*L-V*) relations were characterized with a computer-controlled Keithley 2400 Sourcemeter. The UPS was measured with ThermoFisher.

2.2 Fabrications and Measurements of Inverted OLEDs

Prior to device fabrications, ITO with glass substrate was etched into a specific pattern, and the active device area was 2 mm × 2 mm. Next, the substrate was washed with detergent, deionized water, wiped with ethanol, and sonicated in ethanol solution for 30 min sequentially. At the beginning, the substrate was treated by the O_2-plasma for 5 min under the condition of 120 W. ZnO NPs were spin-coated on a pre-cleaned ITO glass at 2 300 r/min for 40 s and then annealed at 120 ℃ for 10 min in the glove box. Next, the cross-linkable TV-T2T was spin-coated, and the corresponding film was annealed at 150 ℃ for 10 min and then was annealed at 230 ℃ for 30 min. The solution of light-emitting material(2,6-Dczppy: $Ir(mppy)_3$(1∶0.1 wt. ratio)) in chlorobenzene was spin-coated onto the ETL and dried at 80 ℃ for 30 min to remove residual solvent. Finally, 1,1-bis[(di-4-tolylamino) phenyl] cyclohexane (TAPC), hexaazatriphenylenehexacabonitrile (HAT-CN), MoO_3 and Al were sequentially vacuum deposited under the condition of 5×10^{-4} Pa.

2.3 Materials

The ZnO NPs[45] were synthesized through a solution-precipitation process using Zn acetate and tetramethylammonium hydroxide (TMAH) precursors. The reaction process proceeds as follows: a solution of 0.5 mol/L TMAH in ethanol and a solution of 0.1 mol/L zincacetate in dimethyl sulphoxide (DMSO) were mixed and stirred for 1 h in an ambient atmosphere. The prepared product was collected by centrifugation and then washed. The obtained transparent precipitate was dispersed in butanol at a concentration of 20 mg/mL

2.4 Synthesis

2.4.1 Synthesis of The 2,4,6-tris(3-bromophenyl)-1,3,5-triazine(Br-T2T)

3-bromobenzonitrile (11.6 g, 63.7 mmol) was added to a triangular conical flask(250 mL). Then, trifluoromethanesulfonic acid (20.3 mL, 6.7 mmol) was injected into the conical flask with a syringe slowly in an ice bath. The resulting reaction mixture was stirred at 0 ℃ for about 30 min, then slowly warmed to room temperature and stirred for about 12 h. The mixture was finally purified to obtain the Br-T2T as a white solid (10.3 g, 59.3 mmol) (yield: 88.8%): ^{1}H NMR (400 MHz, $CDCl_3$): δ 8.80(t, 1H),8.64(d, 1H), 7.76(d, 1H), 7.46 (t, 1H). ^{13}C (101 MHz, $CDCl_3$): δ 170.64, 137.65, 135.77, 131.84, 130.28, 127.64, 123.03, 77.36. Anal. Calcd for $C_{21}H_{12}N_3Br_3$(%): C 46.19, H 2.22, N 7.7; found: C 46.22, H 2.25, N 7.65.

2.4.2 Synthesis of The Product 2,4,6-tris(4′-vinyl-[1,1′-biphenyl]-3-yl)-1,3,5-triazine (TV-T2T)

Br-T2T(2 g, 3.7 mmol), (4-vinylphenyl) boronic acid (1.91 g, 12.88 mmol), $Pd(PPh_3)_4$ (424 mg, 0.368 mmol) and tert-butylphosphonium tetrafluoroborate(213.6 mg, 0.736 mmol) were added into the 100 mL flask. Then, 1,4-dioxane was added in the flask and stirred to dissolve the Br-T2T. Afterwards, the flask was added with Na_2CO_3 (7.8 g, 73.6 mmol) through a syringe and kept vacuum. Finally, the mixture was heated to 95 ℃ and reacted for 12 h, and purified to get the TV-T2T as a white solid (1.6 g, 2.6 mmol)(yield: 80.0%): ^{1}H NMR (400 MHz, $CDCl_3$) δ 9.00(s, 1H), 8.75(d, 1H), 7.84(d, 1H), 7.72(d, 1H), 7.65(t, 1H), 7.57(d, 1H), 6.81(m, 1H), 5.85(d, 1H), 5.33(d, 1H). ^{13}C NMR(101 MHz, $CDCl_3$) δ 171.68, 141.20, 140.13, 136.97, 136.74, 136.41, 131.10, 129.20, 127.99, 127.48, 127.42, 126.82, 114.17, 77.36, 77.04, 76.73. Anal. Calcd for $C_{45}H_{33}N_3$(%): C 87.77, H 5.41, N 6.82; found: C 87.8, H 5.5, N 6.7.

3 Results and Discussion

The route for TV-T2T synthesis is illustrated in Fig. 1, which was only a two-step reaction process. First, the compound of 3-bromobenzonitrile was reacted under the condition of trifluoromethanesulfonic acid at 0 ℃, and the intermediate 2,4,

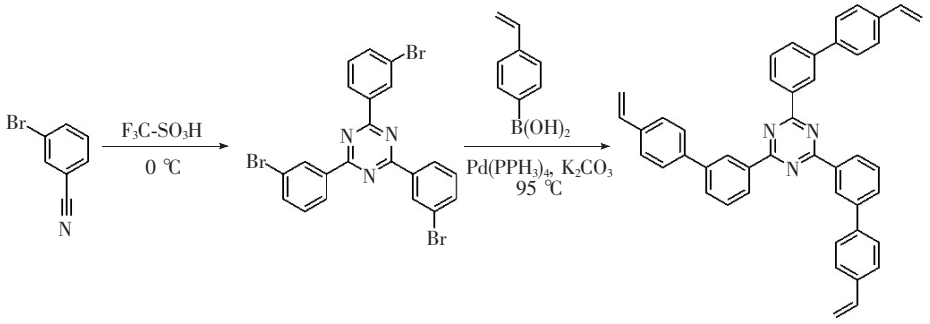

Fig. 1 Synthetic route for TV-T2T

6-tris(3-bromophenyl)-1,3,5-triazine(Br-T2T) was obtained with a yield of 88.8%. Then, the Br-T2T was reacted with (4-vinylphenyl) boronic acid through Suzuki-Miyaura crossing-coupling reaction to reach the target product TV-T2T with a yield of 80.0%. The chemical structures of the Br-T2T and TV-T2T were confirmed by ^{1}H NMR, ^{13}C NMR, and EA.

The photoluminescence(PL) spectra of the TV-T2T films before and after the cross-linking are shown in Fig. 2. The UV-Vis absorption peak positions of the films before and after the cross-linking stayed the same, and the PL peak of the TV-T2T is 446 nm before the cross-linking and 444 nm after the cross-linking, together implying that the cross-linking of TV-T2T would not influence on optical properties for their intrinsic unconjugated linking.

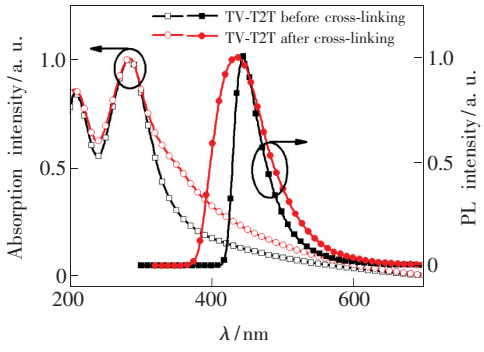

Fig. 2 UV-Vis absorption and PL spectra of the TV-T2T before and after cross-linking

To investigate the properties of the thermal stability, TGA and DSC were carried out for TV-T2T, and the TGA and DSC curves are shown in Fig. 3. They revealed that the polymerization peak was at about 218 ℃, as seen in Fig. 3(a), and the decomposition temperature (T_d) was 430 ℃ (5% weight loss), as seen in Fig. 3(b). After cross-linking, there was no obvious peak, as shown in Fig. 3(b), which showed that the TV-T2T was thermally stable.

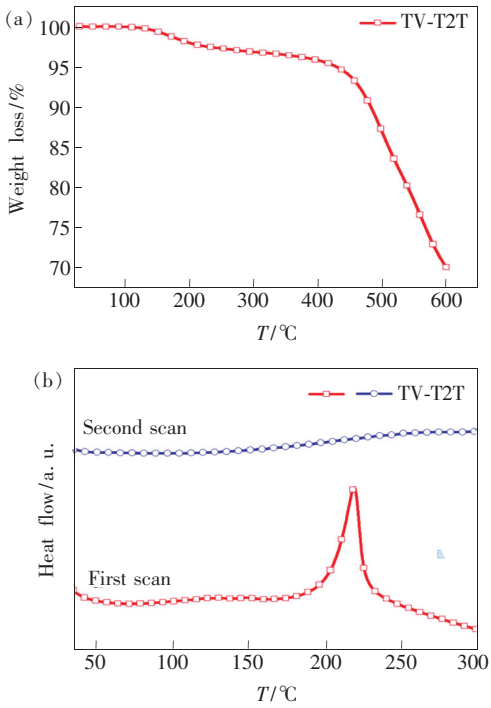

Fig. 3 (a) DSC curve of the material TV-T2T with a heating of 10 ℃/min under nitrogen. (b) TGA curve of the material TV-T2T with a heating rate of 10 ℃/min under nitrogen.

The highest occupied molecular orbit (HOMO) level of the TV-T2T was measured by the Ultraviolet Photoemission Spectroscopy(UPS), which was about −6.5 eV, as shown in Fig. 4. The LUMO of the TV-T2T was approximately −3.5 eV which is lower than that of the conduction band(CB) ZnO (−4.0 eV) and lies between the ZnO layer and the emission layer. Therefore, the TV-T2T as ETL could facilitate the electrons to inject from ZnO to TV-T2T and to the emission layer. All the above

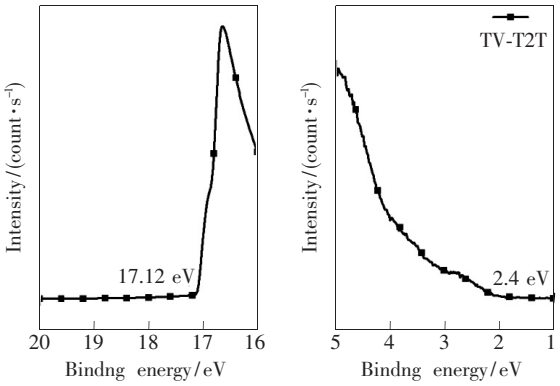

Fig. 4　UPS spectra of TV-T2T

characterization data of TV-T2T are summarized in Tab. 1.

Cross-linked TV-T2T film was measured using UV-Vis spectroscopy on quartz substrates, with toluene, chlorobenzene, tetrahydrofuran and dichloroethane as the testing solvents. The results are shown in Fig. 5(a). The UV-Vis absorptions showed no change before and after rinsing of the TV-T2T films with the solvents, showing that the cross-linked TV-T2T has good resistance to the solvents. In addition, solvent resistance of TV-T2T with various crosslinking conditions were investigated(Fig. 5(b)). It is found that the best crosslinking condition was 220 ℃ for 30 min.

Tab. 1　Thermal and photophysical properties of TV-T2T

Compound	T_{CL}/℃ [a]	T_d/℃ [b]	λ_{abs}/nm [c]	λ_{PL}/nm [c]	HOMO/eV [d]	LUMO/eV	E_g/eV [e]
TV-T2T	218	430	283	444	6.5	3.5	3.0

a Obtained from DSC measurement, b Obtained from TGA measurement, c Measured in thin films by spin-coating from a tetrachloroethane solution, d Calculated from $21.22 - E_k$ from UPS, e Calculated from the edge of the UV-Vis absorption($E_g = 1240/\lambda$).

To investigate the film morphology with the addition of the TV-T2T, four different film compositions were measured by AFM. The films were: (a) ZnO (30 nm), (b) ZnO(30 nm)/TV-T2T(10 nm), (c) ZnO (30 nm)/TV-T2T (10 nm)/2, 6-Dczppy: $Ir(mppy)_3$ (40 nm), and (d) ZnO(30 nm)/2,6-Dczppy:$Ir(mppy)_3$(40 nm). The morphology measurements are shown in Fig. 6. The surface roughness of the ZnO/TV-T2T/$Ir(mppy)_3$ (2.27 nm) was lower than that of the ZnO/2,6-Dczppy: $Ir(mppy)_3$ (2.39 nm), which would reduce the leakage currency. Therefore, it may account for the better efficiency of the device with the TV-T2T in the following results.

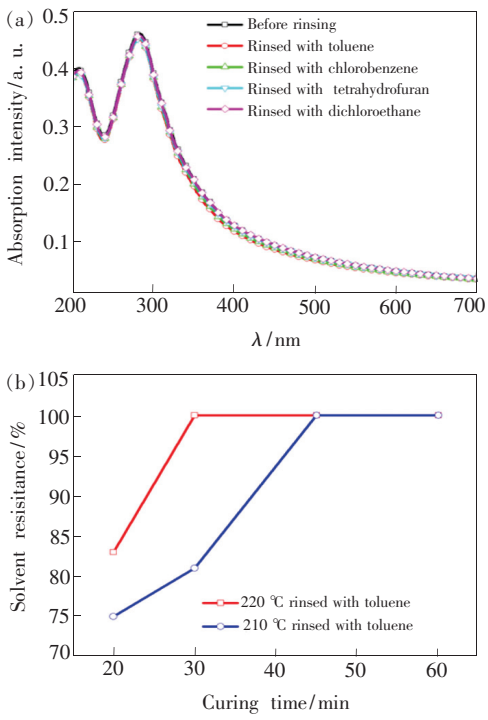

Fig. 5　(a) UV-Vis absorption spectra of the curved TV-T2T films before and after rinsing with toluene, chlorobenzene, tetrahydrofuran and dichloroethane. (b) Solvent resistance of TV-T2T rinsed with toluene at various crosslinking conditions.

To investigate the property of charge injection from the ZnO to TV-T2T, three devices were fabricated

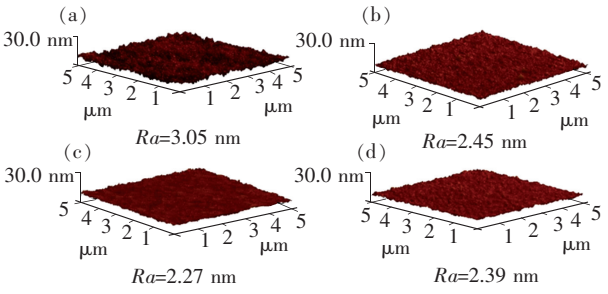

Fig. 6　(a) AFM topographic images of the ZnO(30 nm). (b) AFM topographic images of the ZnO(30 nm)/TV-T2T(10 nm). (c) AFM topographic images of the ZnO(30 nm)/TV-T2T(10 nm)/2,6-Dczppy: $Ir(mppy)_3$(40 nm). (d) AFM topographic images of the ZnO(30 nm)/2,6-Dczppy: $Ir(mppy)_3$(40 nm).

with the TV-T2T and other two commonly used materials, 1,3,5-tris(1-phenyl-1H-benzimidazol-2-yl) benzene(TPBi), and 1,3,5-tri[(3- pyridyl)-phen-3-yl]benzene(TmpyPb), as the ETL, respectively. The structure of the devices consisted of ITO/ZnO (20 nm)/ETL(40 nm)/8-hydroxyquinolinolato-lithium(Liq)(2 nm)/Al(100 nm), for TmPyPb, TPBi, TV-T2T as device 1,2,3 respectively. The measured current densities are shown in Fig. 7. The device fabricated with the TV-T2T as the ETL showed much better performance than the other so that the TV-T2T can effectively improve charge injection efficiency.

Finally, OLEDs were fabricated with the device structure of ITO/ZnO(30 nm)/TV-T2T(x nm)/2,6-Dczppy: Ir(mppy)$_3$(40 nm)/TAPC(30 nm)/HAT-CN(10 nm)/MoO_3(10 nm)/Al(120 nm), as shown in Fig. 8(a). The electron transport layer of

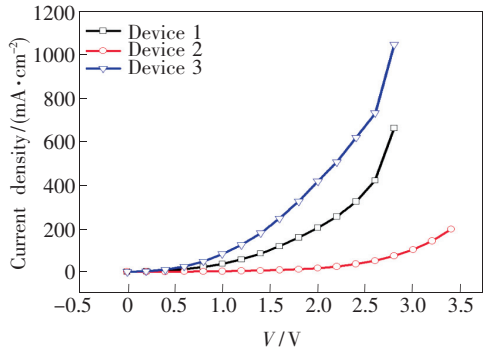

Fig. 7 Current density-voltage of EODs based on the TmPyPb, TPBi and cross-linked TV-T2T.

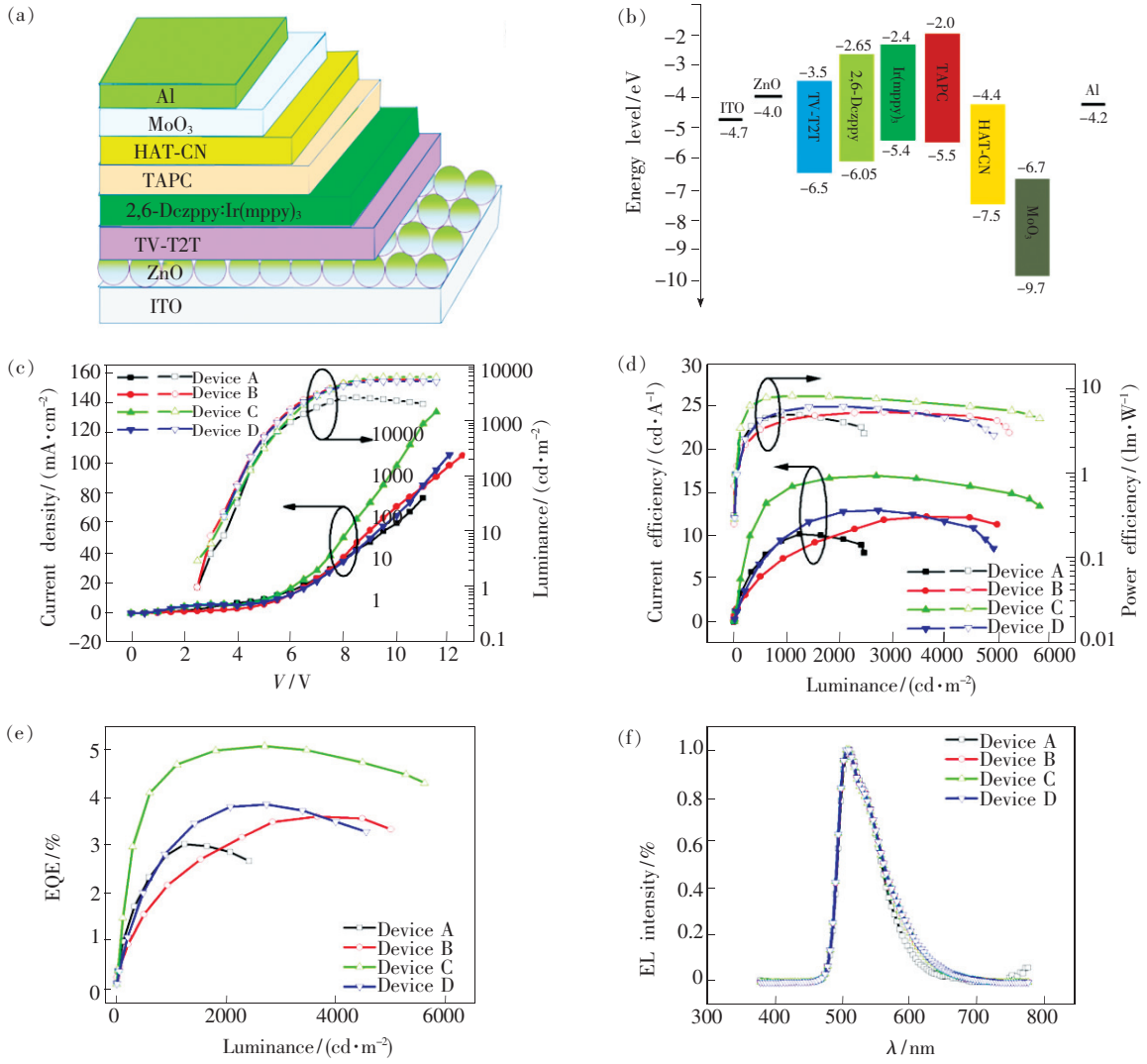

Fig. 8 (a) OLED device structure diagram. (b) Schematic energy-level diagrams. (c) Current density/luminance *vs.* voltage (*J*-*V*-*L*). (d) Current efficiency/power efficiency *vs.* luminance(CE-*L*-PE). (e) Luminance-external quantum efficiency (*L*-EQE). (f) Wavelength-EL intensity.

ZnO and TV-T2T and the emission layer of 2,6-Dczppy: Ir(mppy)$_3$ were fabricated by spin coating. The schematic energy-level diagrams of the solution-processed devices are shown in Fig. 8(b). For optimizations of film thickness of TV-T2T, four different devices were fabricated, namely device A: without two ETL materials based devices, indicating TV-T2T; device B: TV-T2T(5 nm); device C: TV-T2T(10 nm); device D: TV-T2T(15 nm). The device performances are shown in Fig. 8(c) – (f). All the data are summarized in Tab. 2. The device C with a thickness of 10 nm achieved an EQE of 5.1%, a current efficiency(CE) of 16.9 cd/A, a power efficiency(PE) of 8.23 lm/W. In contrast, the device A without the TV-T2T only achieved a maximum EQE of 3.0%, a CE of 10.1 cd/A, a PE of 4.92 lm/W. In terms of EQE, the device with TV-T2T achieved 1.7-fold of improvement compared the device without it.

Tab. 2　EL data of the solution processed OLED

Device	TV-T2T thickness	V_{on} [a]	100 cd/m^2			1 000 cd/m^2			Maximum CE	Maximum PE	Maximum EQE	CIE (x, y)
			CE	PE	EQE	CE	PE	EQE				
A	without	2.5	2.7	1.8	0.8	9.7	4.9	2.8	10.2	4.9	3.0	(0.3, 0.6)
B	5	2.5	2.2	1.6	0.5	7.5	4.3	2.2	12.2	5.3	3.6	(0.3, 0.6)
C	10	2.5	4.0	2.9	1.0	15.3	8.2	4.6	16.9	8.2	5.1	(0.3, 0.6)
D	15	2.5	2.1	1.6	0.6	10.0	5.5	3.0	13.0	6.2	3.9	(0.3, 0.6)

[a]Turn on voltage at 1 cd · m^{-2}; V_{on}: V; thickness: nm; CE: cd · A^{-1}; PE: lm · W^{-1}; EQE: %; Commission Internationale de L'Eclairage (CIE) at 1 000 cd · m^{-2}.

4　Conclusion

A new ETL material, namely TV-T2T, has been designed and synthesized. TV-T2T maintains the best properties of T2T, and in the meantime, possesses good solubility for solution processing and cross-linking units. The LUMO level of TV-T2T (−3.5 eV) lies between the LUMO levels of ZnO (−4.0 eV) and 2,6-Dczppy(−2.6 eV): Ir(mppy)$_3$ (−2.4 eV), which can facilitate efficient charge injection from the ZnO to the 2,6-Dczppy: Ir(mppy)$_3$. Comparing the device without TV-T2T, the surface roughness of TV-T2T based device showed a lower value of 2.27 nm. Using solution processed ZnO/TV-T2T/2,6-Dczppy: Ir(mppy)$_3$ tri-layer architecture, the fabricated OLEDs achieved a maximum EQE of 5.1%. Comparing to a 3.0% EQE of the device without TV-T2T, the tri-layered device delivered 1.7-fold of improvement.

References:

[1] TANG C W, VANSLYKE S A. Organic electroluminescent diodes [J]. *Appl. Phys. Lett.*, 1987, 51(12): 913-915.

[2] LEE C B, UDDIN A, HU X, *et al.*. Study of Alq_3 thermal evaporation rate effects on the OLED [J]. *Mater. Sci. Eng.* B, 2004, 112(1): 14-18.

[3] LEE S, KOO H, CHO S. Mask-less patterning of organic light emitting diodes using electrospray and selective biasing on pixel electrodes [J]. *Appl. Phys. Lett.*, 2015, 106(17): 173303-1-4.

[4] WANG B, WANG Z K, LIANG J, *et al.*. Flash-evaporated small molecule films toward low-cost and flexible organic light-emitting diodes [J]. *J. Mater. Chem.* C, 2017, 5(41): 10721-10727.

[5] YUN W M, JANG J, NAM S, *et al.*. Thermally evaporated SiO thin films as a versatile interlayer for plasma-based OLED passivation [J]. *ACS Appl. Mater. Interfaces*, 2012, 4(6): 3247-3253.

[6] CHEN J X, TAO W W, XIAO Y F, *et al.*. Efficient orange-red thermally activated delayed fluorescence emitters feasible for both thermal evaporation and solution process [J]. *ACS Appl. Mater. Interfaces*, 2019, 11(32): 29086-29093.

[7] 贾克辉, 徐颖, 高劲松, 等. 等离子辅助镀膜技术 [J]. 发光学报, 2002, 23(6): 623-626.
JIA K H, XU Y, GAO J S, *et al.*. Plasma ion assisted deposition for optical coating [J]. *Chin. J. Lumin.*, 2002, 23(6):

623-626. (in Chinese)

[8] ECCHER J, ZAJACZKOWSKI W, FARIA G C, *et al.*. Thermal evaporation versus spin-coating: electrical performance in columnar liquid crystal OLEDs [J]. *ACS Appl. Mater. Interfaces*, 2015, 7(30): 16374-16381.

[9] HU Z, YIN Y, ALI M U, *et al.*. Inkjet printed uniform quantum dots as color conversion layers for full-color OLED displays [J]. *Nanoscale*, 2020, 12(3): 2103-2110.

[10] LIU X, YU Z, YU M J, *et al.*. Iridium(Ⅲ)-complexed polydendrimers for inkjet-printing OLEDs: the influence of solubilizing steric hindrance groups [J]. *ACS Appl. Mater. Interfaces*, 2019, 11(29): 26174-26184.

[11] HU Y X, LIN T, XIA X, *et al.*. Novel phosphorescent iridium(Ⅲ) emitters for both vacuum-deposition and inkjet-printing of OLEDs with exceptionally high efficiency [J]. *J. Mater. Chem.* C, 2019, 7(14): 4178-4184.

[12] WEI C T, ZHUANG J Y, ZHANG D Y, *et al.*. Pyridine-based electron-transport materials with high solubility, excellent film-forming ability, and wettability for inkjet-printed OLEDs [J]. *ACS Appl. Mater. Interfaces*, 2017, 9(44): 38716-38727.

[13] BAN X X, LIU Y, PAN J, *et al.*. Design of blue thermally activated delayed fluorescent emitter with efficient exciton gathering property for high-performance fully solution-processed hybrid white OLEDs [J]. *ACS Appl. Mater. Interfaces*, 2020, 12(1): 1190-1200.

[14] GODUMALA M, YOON J, JEONG C H, *et al.*. An excellent bipolar host material exhibiting EQE of 24.0% with small efficiency roll-off in solution-processable thermally activated delayed fluorescence OLEDs [J]. *J. Mater. Chem.* C, 2019, 7(44): 13930-13938.

[15] PETERS K, RAUPP S, HUMMEL H, *et al.*. Formation of blade and slot die coated small molecule multilayers for OLED applications studied theoretically and by XPS depth profiling [J]. *AIP Adv.*, 2016, 6(6): 065108.

[16] LIU Y, DUZHKO V V, PAGE Z A, *et al.*. Conjugated polymer zwitterions: efficient interlayer materials in organic electronics [J]. *Acc Chem. Res.*, 2016, 49(11): 2478-2488.

[17] PENG F, XU J, ZHANG Y H, *et al.*. Ether-soluble hole-transporting polymers based on triphenylamine/phenothiazine moieties with shallow HOMO levels [J]. *Polym. Chem.*, 2019, 10(11): 1367-1376.

[18] TSAI C E, LIAO M H, CHEN Y L, *et al.*. Triarylamine-based crosslinked hole-transporting material with an ionic dopant for high-performance PEDOT: PSS-free polymer solar cells [J]. *J. Mater. Chem.* C, 2015, 3(24): 6158-6165.

[19] CHENG Y J, LIAO M H, SHIH H M, *et al.*. Exciplex electroluminescence induced by cross-linked hole-transporting materials for white light polymer light-emitting diodes [J]. *Macromolecules*, 2011, 44(15): 5968-5976.

[20] HUANG Q L, EVMENENKO G A, DUTTA P, *et al.*. Covalently bound hole-injecting nanostructures. Systematics of molecular architecture, thickness, saturation, and electron-blocking characteristics on organic light-emitting diode luminance, turn-on voltage, and quantum efficiency [J]. *J. Am. Chem. Soc.*, 2005, 127(29): 10227-10242.

[21] BACHER E, BAYERL M, RUDATI P, *et al.*. Synthesis and characterization of photo-cross-linkable hole-conducting polymers [J]. *Macromolecules*, 2005, 38(5): 1640-1647.

[22] XIE L M, XIONG X Y, CHANG Q W, *et al.*. Inkjet-printed high-efficiency multilayer QLEDs based on a novel crosslinkable small-molecule hole transport material [J]. *Small*, 2019, 15(16): 1900111-1-8.

[23] EARMME T, AHMED E, JENEKHE S A. Solution-processed highly efficient blue phosphorescent polymer light-emitting diodes enabled by a new electron transport material [J]. *Adv. Mater.*, 2010, 22(42): 4744-4748.

[24] YOOK K S, LEE J Y. Solution processed deep blue phosphorescent organic light-emitting diodes with over 20% external quantum efficiency [J]. *Org. Electron.*, 2011, 12(10): 1711-1715.

[25] LEE C W, YOOK K S, LEE J Y. Synthesis and device application of hybrid host materials of carbazole and benzofuran for high efficiency solution processed blue phosphorescent organic light-emitting diodes [J]. *Org. Electron.*, 2013, 14(3): 1009-1014.

[26] EARMME T, JENEKHE S A. High-performance multilayered phosphorescent OLEDs by solution-processed commercial electron-transport materials [J]. *J. Mater. Chem.*, 2012, 22(11): 4660-4668.

[27] YAN X J, TIAN C Y, JIANG W, *et al.*. A scalable seamless full color PMOLED [J]. *J. Soc. Inf. Display*, 2014, 22(5): 245-250.

[28] WANG R, ZHANG D L, XIONG Y, *et al.*. TFT-directed electroplating of RGB luminescent films without a vacuum or mask toward a full-color AMOLED pixel matrix [J]. *ACS Appl. Mater. Interfaces*, 2018, 10(21): 17519-17525.

[29] SONG E, NAM H. Novel voltage programming n-channel TFT pixel circuit for low power and high performance AMOLED displays [J]. *Displays*, 2014, 35(3): 118-125.

[30] LIN C L, CHOU K W, CHANG F C, *et al.*. A novel 3-TFT voltage driving method of compensating V_{TH} shift for a-Si: H TFT and OLED degradation for AMOLED [J]. *Solid State Electron.*, 2011, 64(1): 10-13.

[31] WANG M Y, ZHOU L, YU M J, *et al.*. Amphiphilic conjugated molecules with multifunctional properties as efficient blue emitters and cathode interlayers for inkjet printed organic light-emitting diodes [J]. *J. Mater. Chem.* C, 2017, 5(28): 7075-7083.

[32] XU W D, LAI W Y, HU Q, *et al.*. A hydrophilic monodisperse conjugated starburst macromolecule with multidimensional topology as electron transport/injection layer for organic electronics [J]. *Polym. Chem.*, 2014, 5(8): 2942-2950.

[33] CHEN Y H, LEI Z F, ZHANG X W, *et al.*. Efficient blue organic light-emitting devices based on solution-processed starburst macromolecular electron injection layer [J]. *J. Lumin.*, 2016, 170: 50-55.

[34] XU W D, XIA R D, YE T L, *et al.*. Understanding the light soaking effects in inverted organic solar cells functionalized with conjugated Macroelectrolyte electron-collecting interlayers [J]. *Adv. Sci.*, 2016, 3(2): 1500245-1-7.

[35] LIU X K, ZHENG C J, XIAO J, *et al.*. Novel bipolar host materials based on 1, 3, 5-triazine derivatives for highly efficient phosphorescent OLEDs with extremely low efficiency roll-off [J]. *Phys. Chem. Chem. Phys.*, 2012, 14(41): 14255-14261.

[36] ZHAO B, MIAO Y Q, WANG Z Q, *et al.*. High efficiency and low roll-off green OLEDs with simple structure by utilizing thermally activated delayed fluorescence material as the universal host [J]. *Nanophotonics*, 2016, 6(5): 1133-1140.

[37] LI S W, YU C H, KO C L, *et al.*. Cyanopyrimidine-carbazole hybrid host materials for high-efficiency and low-efficiency roll-off TADF OLEDs [J]. *ACS Appl. Mater. Interfaces*, 2018, 10(15): 12930-12936.

[38] ABDURAHMAN A, CHEN Y X, AI X, *et al.*. A pure red luminescent β-carboline-substituted biphenylmethyl radical: photophysics, stability and OLEDs [J]. *J. Mater. Chem.* C, 2018, 6(42): 11248-11254.

[39] SUZUKI Y, ZHANG Q S, ADACHI C. A solution-processable host material of 1, 3-bis{3-[3-(9-carbazolyl)phenyl]-9-carbazolyl}benzene and its application in organic light-emitting diodes employing thermally activated delayed fluorescence [J]. *J. Mater. Chem.* C, 2015, 3(8): 1700-1706.

[40] CHAPRAN M, PANDER P, VASYLIEVA M, *et al.*. Realizing 20% external quantum efficiency in electroluminescence with efficient thermally activated delayed fluorescence from an exciplex [J]. *ACS Appl. Mater. Interfaces*, 2019, 11(14): 13460-13471.

[41] GOTTARDI S, BARBRY M, COEHOORN R, *et al.*. Efficiency loss processes in hyperfluorescent OLEDs: a kinetic Monte Carlo study [J]. *Appl. Phys. Lett.*, 2019, 114(7): 073301-1-5.

[42] KUO H H, HSU L Y, TSO J Y, *et al.*. Blue-emitting bis-tridentate Ir(Ⅲ) phosphors: OLED performances *vs.* substituent effects [J]. *J. Mater. Chem.* C, 2018, 6(39): 10486-10496.

[43] MO H W, TSUCHIYA Y, GENG Y, *et al.*. Color tuning of avobenzone boron difluoride as an emitter to achieve full-color emission [J]. *Adv. Funct. Mater.*, 2016, 26(37): 6703-6710.

[44] MÉHES G, GOUSHI K, POTSCAVAGE JR W J, *et al.*. Influence of host matrix on thermally-activated delayed fluorescence: effects on emission lifetime, photoluminescence quantum yield, and device performance [J]. *Org. Electron.*, 2014, 15(9): 2027-2037.

[45] BEEK W J, WIENK M M, KEMERINK M, *et al.*. Hybrid zinc oxide conjugated polymer bulk heterojunction solar cells [J]. *J. Phys. Chem.* B, 2005, 109(19): 9505-9516.

高朝(1992 -), 男, 湖北黄冈人, 硕士研究生, 2013 年于湖北工程学院获得学士学位, 主要从事 OLED 材料的合成以及器件等方面的研究。
E-mail: zgao2018@sinano.ac.cn

苏文明(1978 -), 男, 湖南邵东人, 博士, 研究员, 2007 年于中国科学院长春光学精密机械与物理研究所获得博士学位, 主要从事印刷发光与显示等方面的研究
E-mail: wmsu2008@sinano.ac.cn